

DUST CONCENTRATION AND CHONDRULE FORMATION

ALEXANDER HUBBARD¹, MORDECAI-MARK MAC LOW¹, DENTON S. EBEL²

(Dated: November 8, 2018, Revision: 1.20)
Draft version November 8, 2018

ABSTRACT

Meteoritical and astrophysical models of planet formation make contradictory predictions for dust concentration factors in chondrule forming regions of the solar nebula. Meteoritical and cosmochemical models strongly suggest that chondrules, a key component of the meteoritical record, formed in regions with solids-to-gas mass ratios orders of magnitude above background. However, models of dust grain dynamics in protoplanetary disks struggle to surpass factors of a few outside of very brief windows in the lifetime of the dust grains. Worse, those models do not predict significant concentration factors for dust grains the size of chondrule precursors. We briefly develop the difficulty in concentrating dust particles in the context of nebular chondrule formation and show that the disagreement is sufficiently stark that cosmochemists should explore ideas that might revise the concentration factor requirements downwards.

Keywords: Astrophysics – Chondrule formation – Cosmochemistry – Dust dynamics

1. INTRODUCTION

Chondrules are sub-mm melted glassy beads found within chondritic meteorites, generally, although not universally (Urey & Craig 1953; Dullemond et al. 2014), thought to have been generated by melting pre-floating dust grains in the solar nebula. Our understanding of chondritic meteorites and the chondrules they contain remains spectacularly incomplete. Just one of the many fascinating challenges they pose to our understanding of the formation of our solar system and extrasolar planetary systems is the question of dust concentration. Cosmochemists studying chondrules find that they had to have melted in high density regions immensely (factors of hundreds, Wood 1963; Ebel 2006) enriched in condensables above the expected solar ratio (Ebel & Grossman 2000; Tenner et al. 2015). Stabilizing liquids at chondrule melting temperatures requires high partial pressures (Wood 1967). Planetesimal formation and dust coagulation theorists on the other hand wrestle with the need for condensable enrichments of factors of a few (Dubrulle et al. 1995; Birnstiel et al. 2016), and find that when such occur, they require grains larger than chondrules or their precursors, and are generally short lived (Yang et al. 2016).

The question of particle concentration faces two complementary difficulties. On one hand, at the densities assumed in cosmochemical calculations, comparable to or higher than the Minimum Mass Solar Nebula (Hayashi 1981), chondrules and their precursors are small and difficult to concentrate. On the other hand, as the disk evolves gas loss in accretion or winds means that the disk density drops. When the dissipated gas is sufficiently rarefied to allow the concentration of objects the size of chondrule and chondrule precursors, those concentrations are expected to rapidly lead to planetesimal formation (Johansen et al. 2007), and thus be a brief stage in the life time of the dust. In that scenario, one must explain how chondrule formation could strike those narrow windows so precisely.

We adapt dust transport theory for the purposes of the concentration of chondrules and their precursors, and show how

difficult it is to achieve the requested dust concentration factors. This argues for new avenues of research on ways to reduce the required concentration factors. The isotopic measurements of Budde et al. (2016) demonstrate that chondrule melting regions likely contained different material than chondrite assembly regions, and Ebel et al. (2016) show that chondrules have distinctly different overall compositions than the rest of their host meteorite, in particular, less iron. Ebel & Alexander (2011) found major differences in the chondrule chemical outcomes between cases of melting in regions enriched in CI (bulk chondritic meteoritic) material versus melting in regions enriched in chondritic-IDP-like material although the concentration factors considered were on the order of thousands. Similarly, chondrule formation events need not have been in equilibrium as assumed in the calculations of, e.g. Ebel & Grossman (2000). The composition of chondrules might have been kinetically controlled (Nagahara & Ozawa 1996) as long as cooling rates were sufficiently high to cool newly formed chondrules within tens of minutes to hours (Desch & Connolly 2002).

2. MECHANICS OF DUST CONCENTRATION

Protoplanetary disks are expected to support some level of turbulence. Inertial particles are not strictly passive tracers, and turbulent, rather than microphysical, diffusion does have some non-diffusive consequences. For example, preferential concentration concentrates inertial dust grains in high shear-regions between turbulent vortices (Maxey 1987; Cuzzi et al. 2001), while turbulent thermal diffusion, perhaps ill-named, pumps inertial grains from hot regions to cold ones (Hubbard 2016). However, preferential concentration relies on aerodynamically identical particles, and protoplanetary disks have too weak global thermal gradients to be good hosts for turbulent thermal diffusion, so we can approximate dust concentration as the balance between pressure maxima concentrating dust and turbulent diffusion smoothing out those dust concentrations.

Small dust grains in protoplanetary disks are frictionally entrained by the gas with a drag acceleration

$$\left. \frac{\partial \mathbf{v}}{\partial t} \right|_{\text{drag}} = -\frac{\mathbf{v} - \mathbf{u}}{\tau} \quad (1)$$

ahubbard@amnh.org

¹ Dept. of Astrophysics, American Museum of Natural History, New York, NY, USA

² Dept. of Earth and Planetary Sciences, American Museum of Natural History, New York, NY, USA

where \mathbf{v} is the velocity of a dust grain, \mathbf{u} the velocity of the gas at the dust grain's position, and τ the dust grain's frictional stopping time. Grains with radii smaller than the local gas mean free path (which includes chondrules and, absent extreme porosity, their precursors) are in the Epstein drag regime with

$$\tau = \frac{a\rho_\bullet}{\rho_g v_{\text{th}}}, \quad (2)$$

where a and ρ_\bullet are the dust grain's radius and solid density, while ρ_g is the gas density. The gas thermal speed v_{th} is given by

$$v_{\text{th}} \equiv \sqrt{\frac{8k_B T}{\pi m_g}}, \quad (3)$$

where $m_g \simeq 2.3 \text{ amu}$ is the gas mean molecular weight. We also define the Stokes number

$$\text{St} \equiv \tau\Omega, \quad (4)$$

where Ω is the local orbital frequency. Dust grains with $\text{St} \ll 1$, which include chondrules and their precursors, are well coupled to the gas. Thanks to their inverse dependence on ρ_g , τ and St vary strongly spatially and are much smaller in the dense midplane than in the rarefied upper disk atmosphere.

Dust grains with $\text{St} \ll 1$, well coupled to protoplanetary disk gas, drift through said gas towards pressure maxima with a velocity (for an in depth derivation of dust velocities in the presence of gas motion and pressure gradients see, e.g. Hubbard 2016)

$$\mathbf{v} \simeq \frac{\tau}{\rho_g} \nabla p, \quad (5)$$

where p is the gas pressure. As a result of Equation (5), pressure gradients drive dust drift fluxes

$$\mathbf{F}_{\text{drift}} = \rho_d \mathbf{v} \simeq \tau \frac{\rho_d}{\rho_g} \nabla p \quad (6)$$

where ρ_d is the dust fluid density. That flux acts to set up dust concentration maxima in gas pressure maxima. Turbulent diffusion however will act to diffuse away those dust concentration maxima, with a dust diffusive flux

$$\mathbf{F}_{\text{diff}} = -\rho_g \mathbf{D} \nabla \left(\frac{\rho_d}{\rho_g} \right) \quad (7)$$

where \mathbf{D} is the diffusion coefficient. Note that diffusion mixes the dust-to-gas mass ratio

$$\epsilon = \frac{\rho_d}{\rho_g} \quad (8)$$

rather than dust density itself.

In a steady state we have $\mathbf{F}_{\text{drift}} + \mathbf{F}_{\text{diff}} = 0$, which implies

$$\tau \epsilon \nabla p = \rho_g \mathbf{D} \nabla \epsilon. \quad (9)$$

We parameterize the dust diffusion coefficient $\mathbf{D} = \alpha c_s H$ similar to a Shakura & Sunyaev (1973) α -disk, where c_s is the gas adiabatic sound speed. The local pressure scale-height

$$H = \frac{1}{\sqrt{\gamma}} \frac{c_s}{\Omega} = \sqrt{\frac{\pi}{8}} \frac{v_{\text{th}}}{\Omega}, \quad (10)$$

where $\gamma \simeq 1.4$ is the adiabatic index under standard nebular conditions in chondrule forming regions of $R \sim 1 - 2.5$ au

(Boley et al. 2007). Using those definitions for \mathbf{D} and H we can rewrite Equation (9) as

$$\nabla \ln \epsilon = \frac{1}{\sqrt{\gamma}} \frac{\text{St}}{\alpha} \nabla \ln p = \frac{S}{\sqrt{\gamma}} \nabla \ln p, \quad (11)$$

where we have defined $S \equiv \text{St}/\alpha$ following Jacquet et al. (2012). Strictly speaking, converting between an α -disk's α and our own requires consideration of both the Schmidt number and any anisotropy in the turbulent transport but the difference for dust grains of the size we consider is expected to be of order unity (Johansen et al. 2006).

However, from Equation (2) it is clear that in general τ , and hence St and S , decreases with increasing pressure. Accordingly, high pressure regions see smaller drift fluxes, but unchanged diffusive fluxes. Thus it is useful use the identity

$$p = \frac{\rho_g k_B T}{m_g} = \frac{\pi}{8} \rho_g v_{\text{th}}^2 \quad (12)$$

(Eq. 3) to rewrite Equation (11) as

$$\nabla \ln \epsilon = \frac{\pi}{8\sqrt{\gamma}} \frac{a\rho_\bullet \Omega v_{\text{th}}}{\alpha} \frac{\nabla p}{p^2} \leq \frac{\pi}{8\sqrt{\gamma}} \frac{a\rho_\bullet \Omega_M v_{\text{th}M}}{\alpha_m} \frac{\nabla p}{p^2}, \quad (13)$$

where Ω_M , $v_{\text{th}M}$ and α_m are the maximal and minimal Ω , v_{th} , and α over the region of interest, and we intend to integrate from lower pressure (and thus lower ϵ) to higher pressure (and higher ϵ). Integrating Equation (13) from a point 0 with $\epsilon = \epsilon_0$, $p = p_0$, $\tau = \tau_0$ and $v_{\text{th}} = v_{\text{th}0}$ to a point 1 with $\epsilon = \epsilon_1$ and $p = p_0 + \delta p$ we arrive at

$$\ln \left(\frac{\epsilon_1}{\epsilon_0} \right) \leq \frac{\tau_0 \Omega_M}{\sqrt{\gamma} \alpha_m} \frac{v_{\text{th}M}}{v_{\text{th}0}} \left(\frac{\delta p/p_0}{1 + \delta p/p_0} \right). \quad (14)$$

Defining $\text{St}_M \equiv \tau_0 \Omega_M$ and $S_M \equiv \text{St}_M v_{\text{th}M} / \alpha_m v_{\text{th}0}$, Equation (14) simplifies to

$$\ln \left(\frac{\epsilon_1}{\epsilon_0} \right) \leq \frac{S_M}{\sqrt{\gamma}} \left(\frac{\delta p/p_0}{1 + \delta p/p_0} \right) < \frac{S_M}{\sqrt{\gamma}}. \quad (15)$$

We can see that one requires $S_M > 1$ to generate significant variations in the dust-to-gas mass ratio ϵ along a trajectory of interest.

3. DUST CONCENTRATION FACTORS

We consider the case of vertically settled dust further concentrated by a small midplane region of high pressure. When deriving Equation (15) we integrated from low pressure regions to high pressure regions. However, when the high pressure region contains a large fraction of the overall dust mass, as occurs with settling, Equation (15) leaves us with an unknown ϵ_0 . We will invoke the constraint that the vertically integrated dust density equals the dust surface density to solve for ϵ_0 . In practice, this effect mean that even when Equation (15) predicts huge ϵ_1/ϵ_0 ratios, those ratios say more about the extreme dust depletion in the low pressure regions than about the dust concentration in the high pressure ones, which remains modest.

3.1. Settling

In the case of settling we want to integrate Equation (11) from the midplane (i.e. from high pressure to low pressure), and write the mid-plane dust density in terms of the dust surface density. Takeuchi & Lin (2002) did this, deriving the equation for the dust density as a function of altitude in a

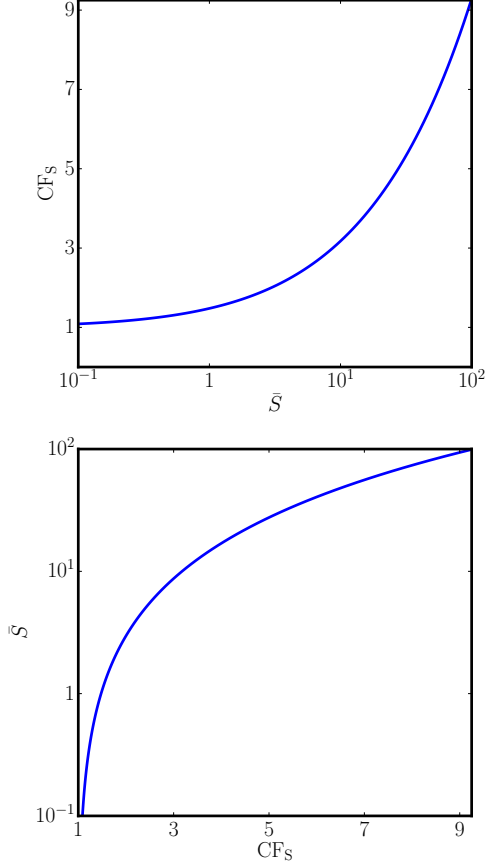


Figure 1. Settling concentration factor CF_S as a function of the midplane \bar{S} and vice-versa for $\gamma = 1.4$. Settling will only drive large concentration factors $CF_S \gtrsim 10$ for $\bar{S} > 10^2$.

constant α , vertically isothermal disk in vertical hydrostatic equilibrium:

$$\rho_g(z) = \rho_g(0) \exp\left(-\frac{z^2}{2H^2}\right), \quad (16)$$

$$\rho_d(z) = \rho_d(0) \exp\left[-\frac{z^2}{2H^2} - \frac{\bar{S}}{\sqrt{\gamma}} \left(\exp \frac{z^2}{2H^2} - 1\right)\right], \quad (17)$$

where \bar{S} is S evaluated at the midplane. Defining

$$I(\bar{S}) \equiv \int_{-\infty}^{+\infty} dz \exp\left[-\frac{z^2}{2H^2} - \frac{\bar{S}}{\sqrt{\gamma}} \left(\exp \frac{z^2}{2H^2} - 1\right)\right] \quad (18)$$

we get the gas and dust surface densities:

$$\Sigma_g = \sqrt{2\pi} H \rho_g(0), \quad (19)$$

$$\Sigma_d = I(\bar{S}) \rho_d(0). \quad (20)$$

In the absence of settling (effectively $S = 0$), we would have $\epsilon = \bar{\epsilon} \equiv \Sigma_d / \Sigma_g$ as the total system dust-to-gas mass ratio.

We can now find that at the midplane

$$\epsilon(\bar{S}, 0) = \frac{\rho_d(0)}{\rho_g(0)} = \frac{\sqrt{2\pi} H}{I(\bar{S})} \bar{\epsilon}. \quad (21)$$

Using Equation (21) we can usefully define the settling con-

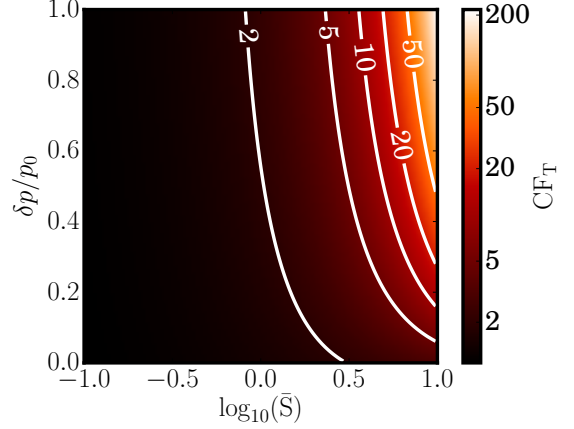


Figure 2. CF_T as a function of \bar{S} and $\delta p/p_0$. We can achieve $CF_T = 10$ for $\bar{S} = 10$ and $\delta p/p_0 = 0.15$.

centration factor at the midplane

$$CF_S(\bar{S}) = \frac{\epsilon(\bar{S}, 0)}{\bar{\epsilon}} = \frac{\sqrt{2\pi} H}{I(\bar{S})}. \quad (22)$$

We plot CF_S as a function of \bar{S} and vice-versa in Figure 1. Note that while settling can lead to large midplane dust concentrations $CF_S \gtrsim 10$, it can only do so for $\bar{S} \gtrsim 10^2$. Even $\bar{S} = 10$ only leads to $CF_S \sim 3$.

3.2. Pressure bump

A radial annulus of high pressure such as a zonal flow (Johansen et al. 2009), or a high pressure anti-cyclonic vortex (Barge & Sommeria 1995) will further concentrate the already settled particles. As long as the region is small enough, the dust mass trapped in the high pressure region will be negligible compared to the total dust mass, and we can use Equation (15) with $\epsilon_0 = \epsilon(\bar{S}, 0)$. Thus, we can define the concentration factor of the pressure bump:

$$CF_p \equiv \frac{\epsilon_1}{\epsilon(\bar{S}, 0)} = \exp\left(\frac{\delta p/p_0}{1 + \delta p/p_0} \frac{\bar{S}}{\sqrt{\gamma}}\right), \quad (23)$$

and the total concentration factor

$$CF_T = \frac{\epsilon_1}{\bar{\epsilon}} = CF_p \times CF_S. \quad (24)$$

In Equation (24) CF_T is explicitly the dust-to-gas mass ratio in the peak of the pressure bump, at the midplane, normalized to the overall system dust-to-gas mass ratio.

We show CF_T as a function of \bar{S} and $\delta p/p_0$ in Figure 2, noting that $CF_T \simeq 10$ for $\bar{S} = 10$ and $\delta p/p_0 = 0.15$. The addition of a pressure bump greatly increases the dust concentration above settling, even though the pressure ratio of the pressure bump is much smaller than that between the disk midplane and the disk upper atmosphere. This is a consequence of our assumption that the pressure bump is sufficiently spatially constrained that it contains only a small fraction of the overall dust mass. This condition can be written as

$$CF_p \times \delta R = \frac{CF_T}{CF_S} \delta R \ll R. \quad (25)$$

for a pressure perturbation with radial extent δR

Table 1
Stokes numbers: MMSN

Chondrules	CV	LL	CM	CO
1 au	1.2e-4	7e-5	3.7e-5	2.1e-5
2.5 au	4.9e-4	2.7e-4	1.5e-4	8e-5
Precursors				
1 au	2.7e-5	1.5e-5	8.1e-6	4.5e-6
2.5 au	1.1e-4	5.9e-5	3.2e-5	1.8e-5

4. APPLICATION TO CHONDRULE PRECURSORS

Our assumption that the pressure bumps are sufficiently spatially localized that they trap only a small fraction of the overall dust mass is highly problematic for chondrule formation purposes. For such pressure perturbations to play a significant role in chondrule formation, they must have been very tightly correlated with chondrule formation mechanisms. Nonetheless, we can examine the consequences of Equation (24) for chondrules and their precursors.

4.1. Stokes numbers

In a vertically isothermal protoplanetary disk, the midplane Stokes number of a dust grain reduces to

$$\text{St} = \frac{\pi a \rho_{\bullet}}{2 \Sigma_g}. \quad (26)$$

Chondrule sizes vary, with typical radii $a = 450, 250, 135, 75 \mu\text{m}$ for CV, LL, CM and CO chondrites respectively (Friedrich et al. 2015). A Hayashi MMSN has surface densities of $\Sigma_g = 1700, 430 \text{ g cm}^{-2}$ at $R = 1, 2.5 \text{ au}$ respectively, while chondrules have solid densities $\rho_{\bullet} \simeq 3 \text{ g cm}^{-3}$. Those numbers result in the Stokes numbers given in Table 1. However, chondrule precursors were presumably porous. At constant mass, $\text{St} \propto \phi^{2/3}$ where ϕ is a porous grain’s volume filling fraction. We will assume that chondrule precursors were only modestly collisionally compacted, with $\phi = 0.1$ (Güttler et al. 2010), resulting in the precursor Stokes numbers also given in Table 1. All of those Stokes numbers are conspicuously low.

In addition to the condensable enrichment, Ebel & Grossman (2000) found a need for high pressure gas in chondrule forming regions, with $p_c \sim 10^{-3} \text{ atm}$, with potential trade-offs between gas pressure and condensable enrichments. Using a mean molecular mass of 2.3 amu (i.e. neglecting any disassociation or ionization) and a temperature of 1750 K , a pressure of $p_c = 10^{-3} \text{ atm}$ corresponds to a gas density of $\rho_g = 1.6 \times 10^{-8} \text{ g cm}^{-3}$. In the limit of the high Mach number required to achieve chondrule forming temperatures from a background of $\sim 300 \text{ K}$, and assuming $\gamma \sim 1.4$, the pre-shock gas would have had a density of $\rho_g \simeq 3 \times 10^{-9} \text{ g cm}^{-3}$ and a thermal speed of $v_{\text{th}} \simeq 1.7 \times 10^5 \text{ cm s}^{-1}$. The corresponding Stokes numbers are given in Table 2, where the R dependence comes from normalizing the stopping time τ to the orbital frequency $\Omega(R)$. Note that if the heating was not due to a shock, the gas would need even higher densities corresponding to even lower St values, and that the Stokes numbers are significantly smaller than in the MMSN case.

4.2. Midplane α and $\delta p/p_0$

Even in the case of magnetically dead midplanes (Gammie 1996) surface layer turbulence will penetrate to the midplane, driving motions (Oishi & Mac Low 2009). While estimates for the strength of that turbulence vary, they generally cluster around $\alpha \gtrsim 10^{-4}$ (Oishi & Mac Low 2009; Bai

Table 2
Pre-shock Stokes numbers assuming post-shock $p_c = 10^{-3} \text{ atm}$

Chondrules	CV	LL	CM	CO
1 au	5.4e-5	3.0e-5	1.6e-5	9e-6
2.5 au	1.4e-5	7.6e-6	4.1e-6	2.3e-6
Precursors				
1 au	1.2e-5	6.5e-6	3.5e-6	1.9e-6
2.5 au	3e-6	1.6e-6	8.9e-7	4.9e-7

2016; Gole et al. 2016). We adopt a conservative estimate of $\alpha \gtrsim 5 \times 10^{-5}$. Note that even in the absence of other forms of turbulence, once low- St dust settles to a concentration factor of ~ 100 , they begin to drive a sufficiently strong Kelvin-Helmholtz instability to prevent further concentration (see e.g. Weidenschilling 2010). Thus, even if there is no external turbulence whatsoever, settling is insufficient to drive high CF_S .

Zonal flows generate pressure perturbations on the order of $\delta p/p_0 \lesssim 0.3$ (Johansen et al. 2009; Dittich et al. 2013). Rossby waves can generate long-lived vortices at the edges of dead-zones with $\delta p/p_0 \lesssim 1$ (Lyra & Mac Low 2012), although the perturbations may not stay at their maximum values for long. In both cases however the pressure perturbation has a sufficient radial extent (a few percent to a few tens of percent the local orbit) that dust concentrations of more than a factor of 10 will begin to involve large fractions of the total disk dust mass.

Indeed, that is the general result. Noting that for $\bar{S} \leq 3$ we have $\text{CF}_S \leq 2$, and a total concentration factor of $\text{CF}_T > 100$ implies (Equation 25):

$$\frac{\delta R}{R} \ll \frac{1}{\text{CF}_p} = \frac{\text{CF}_S}{\text{CF}_T} < \frac{1}{50}. \quad (27)$$

A MMSN has $H/R \sim 1/30$, so to achieve a large CF_T under MMSN-like conditions for $\bar{S} \leq 3$ we need, simultaneously, $\delta p/p_0 > 1$ and $\delta R \ll H$. Such a ‘‘perturbation’’ would generate strong enough outwards pressure forces that the disk’s angular momentum would locally cease to increase with radius, violating the requirement for Rayleigh stability.

4.3. Implications

Porous CV chondrule precursors, in extremely quiescent MMSN midplanes ($\alpha = 5 \times 10^{-5}$) could manage $\bar{S} = 2$ at $R = 2.5 \text{ au}$. Non-porous CM chondrules, in said extremely quiescent MMSN midplanes could approach $\bar{S} = 3$ at $R = 2.5 \text{ au}$. CO chondrules, much less CO chondrule precursors, struggle to match $\bar{S} = 1$. If we want the pressure in chondrule forming regions to approach $p_c = 10^{-3} \text{ atm}$, then $\bar{S} > 1$ is ruled out in all but the most optimistic of cases (extremely quiescent midplanes, close to $R = 1 \text{ au}$, non-porous precursors of the largest chondrules).

We can trade off the MMSN approximation for an α -disk one by returning to the mass accretion rate for a constant α disk (Frank et al. 2002):

$$\dot{m} = 3\pi\alpha_{\text{eff}}c_s\Sigma_g H. \quad (28)$$

Inserting Equation (28) into Equation (26) we arrive at

$$S \simeq 0.76 \left(\frac{a\rho_{\bullet}}{0.135 \text{ g cm}^{-2}} \right) \left(\frac{\dot{m}}{10^{-8} \text{ M}_{\odot} \text{ yr}^{-1}} \right)^{-1} \times \left(\frac{\alpha}{\alpha_{\text{eff}}} \right)^{-1} \left(\frac{R}{2.5 \text{ au}} \right)^{3/2}, \quad (29)$$

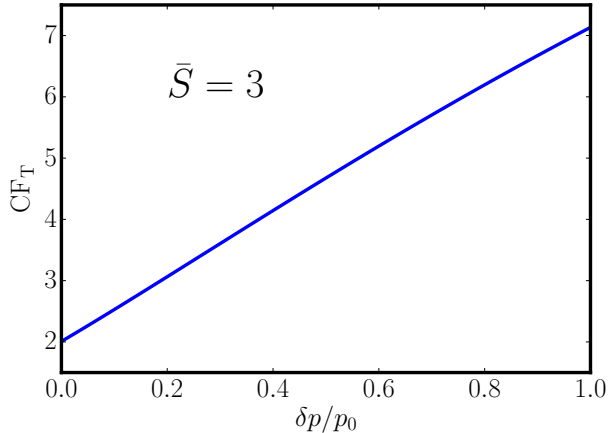


Figure 3. CF_T as a function of $\delta p/p_0$ for $\bar{S} = 3$, where we have normalized $\alpha\rho_\bullet$ to large non-porous CV chondrules. Quiescent T Tauri stars accrete at around $10^{-8} M_\odot \text{ yr}^{-1}$ (Ingleby et al. 2013) although values closer to $10^{-9} M_\odot \text{ yr}^{-1}$ occur. While the link between the midplane dust diffusion coefficient α and the accretion driving α_{eff} is unclear, it is difficult to imagine $\alpha < 0.1\alpha_{\text{eff}}$. Thus, we are still left with CO chondrule precursors having $\bar{S} < 3$ even in the most optimistic of cases.

We cannot achieve even merely $CF_T = 10$ with these maximal estimates for $\bar{S} \leq 3$ as shown in Figure 3, noting further that $\delta p/p_0$ is not expected to be large. Thus, we find ourselves with predictions of $CF_T < 10$ for chondrules and chondrule precursors under all conditions except perhaps for CV chondrules (not precursors) at $R = 2.5 \text{ au}$ in an extremely quiescent disk ($\alpha = 5 \times 10^{-5}$) with very strong long-lived pressure perturbations ($\delta p/p_0 = 0.15$). Some further intermittent concentration is possible: perhaps a factor of 6 from a strong shock, and a factor of 2 from preferential concentration (Hubbard 2013), but final factors of hundreds, or even tens, are not expected.

5. FURTHER COMPLICATIONS

5.1. Non-concentrated dust

In the calculations above we explicitly assumed that most of the dust mass is not in the regions of peak concentration. In that model, most heating events strong enough to melt chondrules should have hit non-concentrated dust unless the heating mechanism was tightly linked to the pressure perturbation concentrating the dust. Requiring that large fractions of the dust mass be in dense clumps greatly increases the difficulty in concentrating the dust, and is inconsistent with observations: we see dust almost everywhere in protoplanetary disks with gaps being the exciting exception (ALMA Partnership et al. 2015). Relaxing this assumption reduces the amount of dust in the regions of peak concentration: there is not an arbitrary amount of dust available to parcel out to the pressure maxima. This is the reason why the vast pressure ratios between the upper disk atmosphere and the disk midplane only generate dust concentration factors comparable to much more moderate midplane pressure perturbations of tens of percents.

5.2. Concentrated dust

While as we have shown one does not expect strong concentrations of chondrules or their precursors we can also examine

the conditions required for strong concentrations. From Figure 2, we could reasonably get $CF_T \gtrsim 10$ for $\bar{S} \gtrsim 10$ and $\delta p/p_0 = 0.15$. Given a moderate estimate for a laminar disk midplane of $\alpha = 10^{-4}$ that implies $St \gtrsim 10^{-3}$. Yang et al. (2016) find that those concentrations and Stokes numbers lead to the streaming instability (Youdin & Goodman 2005), which can rapidly create dense, gravitationally unstable dust clouds. Thus, concentrations $CF_T \gtrsim 10$ are not expected to be long lived, but instead to be a brief stage in the process of planetesimal formation. In that case, it becomes difficult to imagine why chondrule forming events would strike only during such a brief window in the dust’s life, and it is difficult to see how matrix material (much of which stayed well below chondrule forming temperatures) would have had time to be evenly mixed in with the newly formed chondrules before planetesimal formation finalized.

Strong radial pressure perturbations concentrate dust grains in pressure maxima, regions with zero radial pressure gradients, and so do not host the streaming instability. However, this also means that concentrated dust layers do not trigger Kelvin-Helmholtz instabilities, allowing the classical Safronov-Goldreich-Ward gravitational instability (Safronov 1969; Goldreich & Ward 1973). Thus, high dust concentration requirements find themselves on the horns of a dilemma: chondrule precursors are not expected to have been strongly concentrated, but even if they were, those concentrations are not expected to have lasted long enough to allow chondrule formation events to preferentially strike them.

5.3. Concentration times scales

Our concentration analyses in Sections 2 and 3 assume equilibrium between dust drift and turbulence. The vertical settling time of $t \sim 1/2\pi St$ local orbits is short compared to disk lifetimes for all but the smallest grains considered in Table 1 or 2, but the same is not true for concentration in radial pressure bumps. Radial drift in an MMSN-like disk occurs at a speed of approximated

$$v_{\text{drift}} \simeq 50St \text{ m/s} \simeq 10^{-2}St \text{ au/yr.} \quad (30)$$

Assuming dust concentrates from an annulus of width ΔR final annulus of width δR , to achieve the concentration factor $CF_p = 50$ assumed in Equation (27) one requires

$$\frac{\Delta R}{R} \simeq \left[\sqrt{100 \frac{\delta R}{R} + 1} - 1 \right] \quad (31)$$

where we have already assumed $\delta R \ll R$. For the smallest reasonable annulus width $\delta R/R \simeq H/R \sim 1/30$, Equation (31) implies $\Delta R \simeq R > 1 \text{ au}$ and hence a drift time greater than $100St^{-1}$ years. For the values in Tables 1 and 2, this ranges from 200 kyr in the most generous case up to 200 myr in the least generous case. It is hard to imagine a radial pressure perturbation remaining unmodified for such a long time even in the most optimistic of cases.

6. CONCLUSIONS

We have examined the requirement for strong dust concentration in protoplanetary disks finding that chondrule precursors are not expected to have been concentrated even by a single order of magnitude. That is in strong tension with cosmochemical analyses that find chondrule forming events had to have occurred in regions with dust concentrations of factors of hundreds to thousands (Ebel & Grossman 2000;

Tenner et al. 2015). While the details depend on the overall disk density, the higher the density, the harder it is to concentrate dust. We have examined both the $p = 10^{-3}$ atm case preferred by cosmochemists and the significantly lower density Hayashi MMSN Solar Nebula (Ebel & Grossman 2000; Hayashi 1981), finding that both are too dense to allow significant dust concentration. While sufficiently rarified gas to allow high dust concentration factors are expected late in a protoplanetary disk's life, they are faced with a separate problem. Dynamical theory predicts that if and when extremely high dust concentrations are achieved, they are but brief stages in dust evolution, lasting significantly less than 1000 yr, and culminating in the formation of planetesimals through collective instabilities such as the streaming instability (Youdin & Goodman 2005). Even if such concentrations of chondrule precursors were possible it is therefore difficult to imagine how they could have been sufficiently correlated with chondrule forming events.

Most of the disk cannot (by definition) have extremely high dust concentrations. High dust concentrations in chondrule forming events therefore requires that chondrule forming events either have caused or been caused by high dust concentrations, and that those concentrations not have led to rapid planetesimal formation or accretion onto planetesimals. Dynamical concentration of chondrule sized dust appears ruled out outside of the very end of the disk's lifetime, and when it is possible, dust concentration naturally leads to planetesimal formation. The goal posts for nebular high dust concentration chondrule formation are thus extremely narrow. Chondrite classes are sufficiently numerous that absent a large chondrite class-to-planetesimal ratio (e.g. Weiss & Elkins-Tanton 2013), invoking extremely rare conditions is disfavored. We seem to be left with discarding either "nebular" or "high concentration" in chondrule formation.

This concentration contradiction provides an exciting way to link cosmochemistry to disk dynamics and to learn from both. The cosmochemical requirements are sufficiently distant from the dynamical predictions, and turbulent diffusion of passive scalars is a sufficiently well understood problem, that the cosmochemical constraints need to be revisited, perhaps varying dust compositions (Ebel et al. 2016) or appealing to kinetic effects (Nagahara & Ozawa 1996). If no alternatives with strongly lowered condensable concentrations can be found, we will need to rethink our understanding of protoplanetary disks and dust transport therein at a fundamental level, or to adopt non-nebular models of chondrule formation (Urey & Craig 1953).

ACKNOWLEDGEMENTS

We thank Stu Weidenschilling and an anonymous referee for their useful comments, suggestions, and elaborations on the difficulties we present here. The research leading to these results was funded by NASA OSS grant NNX14AJ56G (AH) and EW grant NNX16AD37G (DE).

REFERENCES

- ALMA Partnership et al. 2015, The 2014 ALMA Long Baseline Campaign: First Results from High Angular Resolution Observations toward the HL Tau Region, *ApJ*, 808, L3
- Bai, X.N. 2016, Towards a Global Evolutionary Model of Protoplanetary Disks, *ApJ*, 821, 80
- Barge, P. and Sommeria, J. 1995, Did planet formation begin inside persistent gaseous vortices?, *A&A*, 295, L1
- Birnstiel, T., Fang, M. and Johansen, A. 2016, Dust Evolution and the Formation of Planetesimals, *Space Sci. Rev.*, 205, 41
- Boley, A.C. et al. 2007, The Internal Energy for Molecular Hydrogen in Gravitationally Unstable Protoplanetary Disks, *ApJ*, 656, L89
- Budde, G. et al. 2016, Tungsten isotopic constraints on the age and origin of chondrules, *Proceedings of the National Academy of Science*, 113, 2886
- Cuzzi, J.N. et al. 2001, Size-selective Concentration of Chondrules and Other Small Particles in Protoplanetary Nebula Turbulence, *ApJ*, 546, 496
- Desch, S.J. and Connolly, Jr., H.C. 2002, A model of the thermal processing of particles in solar nebula shocks: Application to the cooling rates of chondrules, *Meteoritics and Planetary Science*, 37, 183
- Dittrich, K., Klahr, H. and Johansen, A. 2013, Gravoturbulent Planetesimal Formation: The Positive Effect of Long-lived Zonal Flows, *ApJ*, 763, 117
- Dubulle, B., Morfill, G. and Sterzik, M. 1995, The dust subdisk in the protoplanetary nebula, *Icarus*, 114, 237
- Dullemond, C.P., Stammer, S.M. and Johansen, A. 2014, Forming Chondrules in Impact Splashes. I. Radiative Cooling Model, *ApJ*, 794, 91
- Ebel, D.S. 2006, Condensation of Rocky Material in Astrophysical Environments, ed. D. S. Lauretta & H. Y. McSween, 253–277
- Ebel, D.S. and Alexander, C.M.O. 2011, Equilibrium condensation from chondritic porous IDP enriched vapor: Implications for Mercury and enstatite chondrite origins, *Planet. Space Sci.*, 59, 1888
- Ebel, D.S. et al. 2016, Abundance, major element composition and size of components and matrix in CV, CO and Acfer 094 chondrites, *Geochim. Cosmochim. Acta*, 172, 322
- Ebel, D.S. and Grossman, L. 2000, Condensation in dust-enriched systems, *Geochim. Cosmochim. Acta*, 64, 339
- Frank, J., King, A. and Raine, D.J. 2002, *Accretion Power in Astrophysics: Third Edition*, 398
- Friedrich, J.M. et al. 2015, Chondrule size and related physical properties: A compilation and evaluation of current data across all meteorite groups, *Chemie der Erde / Geochemistry*, 75, 419
- Gammie, C.F. 1996, Layered Accretion in T Tauri Disks, *ApJ*, 457, 355
- Goldreich, P. and Ward, W.R. 1973, The Formation of Planetesimals, *ApJ*, 183, 1051
- Gole, D. et al. 2016, Turbulence, Transport, and Waves in Ohmic Dead Zones, *ApJ*, 826, 18
- Güttler, C. et al. 2010, The outcome of protoplanetary dust growth: pebbles, boulders, or planetesimals?. I. Mapping the zoo of laboratory collision experiments, *A&A*, 513, A56
- Hayashi, C. 1981, Structure of the Solar Nebula, Growth and Decay of Magnetic Fields and Effects of Magnetic and Turbulent Viscosities on the Nebula, *Progress of Theoretical Physics Supplement*, 70, 35
- Hubbard, A. 2013, Turbulence-induced collision velocities and rates between different sized dust grains, *MNRAS*, 432, 1274
- . 2016, Turbulent thermal diffusion: a way to concentrate dust in protoplanetary discs, *MNRAS*, 456, 3079
- Ingleby, L. et al. 2013, Accretion Rates for T Tauri Stars Using Nearly Simultaneous Ultraviolet and Optical Spectra, *ApJ*, 767, 112
- Jacquet, E., Gounelle, M. and Fromang, S. 2012, On the aerodynamic redistribution of chondrite components in protoplanetary disks, *Icarus*, 220, 162
- Johansen, A., Klahr, H. and Mee, A.J. 2006, Turbulent diffusion in protoplanetary discs: the effect of an imposed magnetic field, *MNRAS*, 370, L71
- Johansen, A. et al. 2007, Rapid planetesimal formation in turbulent circumstellar disks, *Nature*, 448, 1022
- Johansen, A., Youdin, A. and Klahr, H. 2009, Zonal Flows and Long-lived Axisymmetric Pressure Bumps in Magnetorotational Turbulence, *ApJ*, 697, 1269
- Lyra, W. and Mac Low, M.M. 2012, Rossby Wave Instability at Dead Zone Boundaries in Three-dimensional Resistive Magnetohydrodynamical Global Models of Protoplanetary Disks, *ApJ*, 756, 62
- Maxey, M.R. 1987, The gravitational settling of aerosol particles in homogeneous turbulence and random flow fields, *Journal of Fluid Mechanics*, 174, 441
- Nagahara, H. and Ozawa, K. 1996, Evaporation of forsterite in H₂ gas, *Geochim. Cosmochim. Acta*, 60, 1445
- Oishi, J.S. and Mac Low, M.M. 2009, On Hydrodynamic Motions in Dead Zones, *ApJ*, 704, 1239
- Safronov, V.S. 1969, *Evolutsiia doplanetnogo oblaka*.
- Shakura, N.I. and Sunyaev, R.A. 1973, Black holes in binary systems. Observational appearance., *A&A*, 24, 337
- Takeuchi, T. and Lin, D.N.C. 2002, Radial Flow of Dust Particles in Accretion Disks, *ApJ*, 581, 1344
- Tenner, T.J. et al. 2015, Oxygen isotope ratios of FeO-poor chondrules in CR3 chondrites: Influence of dust enrichment and H₂O during chondrule formation, *Geochim. Cosmochim. Acta*, 148, 228

- Urey, H.C. and Craig, H. 1953, The composition of the stone meteorites and the origin of the meteorites, *Geochim. Cosmochim. Acta*, 4, 36
- Weidenschilling, S.J. 2010, Particles in the nebular midplane: Collective effects and relative velocities, *Meteoritics and Planetary Science*, 45, 276
- Weiss, B.P. and Elkins-Tanton, L.T. 2013, Differentiated Planetesimals and the Parent Bodies of Chondrites, *Annual Review of Earth and Planetary Sciences*, 41, 529
- Wood, J.A. 1963, On the Origin of Chondrules and Chondrites, *Icarus*, 2, 152
- . 1967, Olivine and pyroxene compositions in type II carbonaceous chondrites, *Geochim. Cosmochim. Acta*, 31, 2095
- Yang, C.C., Johansen, A. and Carrera, D. 2016, Concentrating small particles in protoplanetary disks through the streaming instability, *ArXiv e-prints*
- Youdin, A.N. and Goodman, J. 2005, Streaming Instabilities in Protoplanetary Disks, *ApJ*, 620, 459